HHS Public Access

Author manuscript

Ann Eye Sci. Author manuscript; available in PMC 2021 July 20.

Published in final edited form as:

Ann Eye Sci. 2021 March ; 6: . doi:10.21037/aes-2021-01.

Characteristics of normal human retinal pigment epithelium cells with extremes of autofluorescence or intracellular granule count

Katharina Bermond[1,2], **Andreas Berlin**[1], **Ioana-Sandra Tarau**[1], **Christina Wobbe**[1], **Rainer Heintzmann**[3,4], **Christine A. Curcio**[5], **Kenneth R. Sloan**[5], **Thomas Ach**[6]

[1]Department of Ophthalmology, University Hospital Würzburg, Würzburg, Germany;

[2]Department of Ophthalmology, Ludwigshafen Hospital, Ludwigshafen, Germany;

[3]Leibniz Institute of Photonic Technology, Jena, Germany;

[4]Institute of Physical Chemistry and Abbe Center of Photonics, Friedrich-Schiller University Jena, Jena, Germany;

[5]Department of Ophthalmology, University of Alabama at Birmingham, Birmingham, AL, USA;

[6]Department of Ophthalmology, University Hospital Bonn, Bonn, Germany

Abstract

Background: Cells of the retinal pigment epithelium (RPE) accumulate different kinds of granules (lipofuscin, melanolipofuscin, melanosomes) within their cell bodies, with lipofuscin and melanolipofuscin being autofluorescent after blue light excitation. High amounts of lipofuscin granules within the RPE have been associated with the development of RPE cell death and age-related macular degeneration (AMD); however, this has not been confirmed in histology so far. Here, based on our previous dataset of RPE granule characteristics, we report the characteristics of

Correspondence to: Thomas Ach, MD, FEBO. Department of Ophthalmology, University Hospital Bonn, Ernst Abbe Straße 2, Bonn, 53127, Germany. thomas.ach@ukbonn.de.

Contributions: (I) Conception and design: K Bermond, KR Sloan, T Ach; (II) Administrative support: K Bermond, T Ach; (III) Provision of study materials or patients: CA Curcio, R Heintzmann, KR Sloan, T Ach; (IV) Collection and assembly of data: K Bermond, A Berlin, C Wobbe, IS Tarau, CA Curcio, R Heintzmann, T Ach; (V) Data analysis and interpretation: K Bermond, A Berlin, CA Curcio, T Ach; (VI) Manuscript writing: All authors; (VII) Final approval of manuscript: All authors.

Reporting Checklist: The authors have completed the MDAR reporting checklist. Available at http://dx.doi.org/10.21037/aes-2021-01

Data Sharing Statement: Available at http://dx.doi.org/10.21037/aes-2021-01

Conflicts of Interest: The authors have completed the ICMJE uniform disclosure form (available at http://dx.doi.org/10.21037/aes-2021-01). The series “Retinal Imaging and Diagnostics” was commissioned by the editorial office without any funding or sponsorship. Dr. Heintzmann reports grants from NIH/NEI 1R01EY027948, during the conduct of the study. Dr. Curcio reports grants from NEI/NIH 1R01EY06109, grants from NEI/NIH 1R01EY027948, during the conduct of the study; grants from Heidelberg Engineering, grants from Genentech/Hoffman LaRoche, other from MacRegen Inc, outside the submitted work. Dr. Sloan reports other from MacRegen, outside the submitted work. Dr. Ach reports grants from NIH/NEI 1R01EY027948, grants from Dr Werner Jackstädt Foundation, other from MacRegen, during the conduct of the study. The authors have no other conflicts of interest to declare.

Ethical Statement: The authors are accountable for all aspects of the work in ensuring that questions related to the accuracy or integrity of any part of the work are appropriately investigated and resolved. The study was conducted in accordance with the Declaration of Helsinki (as revised in 2013). The study was approved by institutional review boards of the University of Alabama at Brimingham and University of Würzburg (NO.: 208/15). Due to its retrospective character, informed consent was waived from all participants.

RPE cells from human donor eyes that show either high or low numbers of intracellular granules or high or low autofluorescence (AF) intensities.

Methods: RPE flatmounts of fifteen human donors were examined using high-resolution structured illumination microscopy (HR-SIM) and laser scanning microscopy (LSM). Autofluorescent granules were analyzed regarding AF phenotype and absolute number of granules. In addition, total AF intensity per cell and granule density (number of granules per cell area) were determined. For the final analysis, RPE cells with total granule number below 5th or above the 95th percentile, or a total AF intensity ± 1.5 standard deviations above or below the mean were included, and compared to the average RPE cell at the same location. Data are presented as mean ± standard deviation.

Results: Within 420 RPE cells examined, 42 cells were further analyzed due to extremes regarding total granule numbers. In addition, 20 RPE cells had AF 1.5 standard deviations below, 28 RPE cells above the mean local AF intensity. Melanolipofuscin granules predominate in RPE cells with low granule content and low AF intensity. RPE cells with high granule content have nearly twice (1.8 times) as many granules as an average RPE cell.

Conclusions: In normal eyes, outliers regarding autofluorescent granule load and AF intensity signals are rare among RPE cells, suggesting that granule deposition and subsequent AF follows intrinsic control mechanisms at a cellular level. The AF of a cell is related to the composition of intracellular granule types. Ongoing studies using AMD donor eyes will examine possible disease related changes in granule distribution and further put lipofuscińs role in aging and AMD further into perspective.

Keywords

Retinal pigment epithelium (RPE); granules; autofluorescence (AF); lipofuscin; melanolipofuscin; melanosomes

Introduction

The retinal pigment epithelium (RPE) cell layer is embedded between the photoreceptors and the Bruch membrane. It is a monolayer of polygonal cells that play important roles in maintaining outer retinal health, protein and oxygen transport, and in the phagocytosis of shed photoreceptor outer segments. RPE cells incorporate different kinds of pigmented and non-pigmented organelles of imaging significance (granules): lipofuscin (L), melanolipofuscin (ML), melanosomes (M), and mitochondria (MC) (1). Some of them, L and ML, are autofluorescent after excitation with blue light (2,3).

Blue light fundus autofluorescence (FAF) is widely used in routine clinical diagnostics and disease monitoring (4,5); however, the histological basis of FAF and age-related as well as disease-related autofluorescence (AF) have been investigated only recently (6,7). We added information on histological RPE AF, showing that RPE AF depends on retinal position in relation to the fovea and age. Despite the significant increase in AF, RPE cells maintain a continuous monolayer, though individual RPE cell geometry might change (i.e., cell shape, number of neighbors). In degenerative diseases like age-related macular degeneration (AMD), RPE cells overall tend to lose AF due to loss of autofluorescent granules, although

there are intensely hyperautofluorescent regions within cells, due to granule aggregation. This diminution of AF in AMD has been shown both in *ex vivo* histology (8) and *in vivo* quantitative FAF (9,10).

Recently, we further classified >195,000 intracellular RPE granules (L, ML, M) within 450 RPE cells based on their autofluorescent properties using high-resolution structured illumination microscopy (HR-SIM) (11). A major finding was that the major contributor to AF at the fovea is the relative high ML load within foveal RPE cells, while L dominate RPE cells at the perifovea. RPE cells can incorporate hundreds of intracellular granules, while still maintaining geometric precision, suggesting that they are healthy and highly functional.

Previous reports suggested that high AF and massive load of L granules within RPE cells is a precursor of AMD or AMD related changes (12). However, subsequent histological studies of human eyes, both in normal aging and in AMD (8,13,14) eyes provided no evidence for this theory of L-instigated RPE cell death.

Here, to further support the idea that granule load within RPE cells is well-regulated and organized we hypothesized that RPE cells at the upper and lower end in granule load or AF will not markedly differ from an average RPE cell. Based on our previous data on characterization and number of intracellular granules within RPE cells, we analyzed those RPE cells with high/low granule load or high/low total AF regarding their retinal location, cell size, intracellular granule density, and relation to age. We present the following article in accordance with the MDAR reporting checklist (available at http://dx.doi.org/10.21037/aes-2021-01).

Methods

The study was conducted in accordance with the Declaration of Helsinki (as revised in 2013) and the Harmonized Tripartite Guideline for Good Clinical Practice from the International Conference on Harmonization. The use of human tissue was approved by the Institutional Review Boards of the University of Alabama at Birmingham and the University of Würzburg (208/15). Due to its retrospective character, individual consent was waived.

Tissue preparation and imaging

Tissue collection, preparation, and granule counts within RPE cells is based on 15 RPE/BrM flat mounts (15 Caucasian donors; eight ≤51 years, seven >80 years), as previously reported (11,13).

In brief, globes were collected from the Advancing Sight Network (formerly the Alabama Eye Bank; Birmingham, AL, USA), and inspected under a dissection microscope to exclude macular or retinal pathologies. The neuroretina and choroid were removed in a multistep preparation and imaging process to ensure preservation of the exact foveal position (13). RPE/BrM flat mounts were imaged using a laser scanning confocal fluorescence microscope (LSM) and a structured illumination microscope (SIM). Excitation wavelength was set at 488 nm for both microscopes and AF emission recorded from 490 to 695 nm in 24 channels (LSM), or between 510 and 750 nm (SIM), respectively. The scans were conducted from

apical RPE (first granules in focus) to basal RPE (last granules out of focus), representing the cushion of granules, in 390 nm (LSM) or 110 nm steps (SIM), respectively. Identical areas were imaged at three predefined locations: fovea, superior perifovea, and near-periphery at the superior edge of the flat mount (11,13).

Cell selection and granule classification

Using custom FIJI plugins (https://fiji.sc) (15), at each location, 10 adjacent cells were selected from reconstructed SIM images, and on LSM images the identical cells were marked (10 cells/location for each of the 15 donors = 450 cells), as previously described. Three foveas (donor ages 36, 82, and 88 years) were excluded from the current analysis since RPE cell boundaries were not clearly detectable, resulting in 420 RPE cells for final analysis.

Within SIM images, all detectable granules within the RPE cell bodies were manually tagged and classified on the basis of granule morphology. Nine different phenotypes were identified based on the AF pattern and structural properties [for details see Figure 1 in Bermond *et al.* (11)] using a custom written FIJI plugin. For each tagged granule, the classification code and its x, y, z coordinates within the stack were registered. In the current study, we distinguish only among the classic three intracellular RPE granule classes: Lipofuscin granules (L, nearly spherical granules with homogenous hyper-AF), Melanolipofuscin granules (ML, round or spindle-shaped granules with iso- to hypo-AF core and hyper-AF coating) and Melanosomes (M, hypo-AF round or spindle shaped granules without hyper-AF coating). Using LSM images from the identical cells, total AF per cell (AF intensity expressed as a planimetric density) was calculated.

Analysis of RPE cell bodies with high/ low granule content or high/low AF-intensity

To identify cells with remarkably high or low granule content, total number of granules was calculated for each of the 420 cells. Cells with a granule content below the 5^{th} or above the 95^{th} percentile were selected for this study. Absolute numbers of M, L and ML as well as mean AF-intensity per cell and cell area are reported. Also, for each cell, the (M+ML)/L-ratio was calculated.

To identify and characterize cells with high or low AF-intensity, mean AF per cell ± standard deviation for each location were calculated and only cells at one specific location within one donor were compared since our LSM imaging setting does not qualify for quantitative AF measurements between locations and donors. Thus, cells with an AF-intensity 1.5 standard deviations higher or lower than the mean AF of the ten cells at a specific location were selected for further analysis. For each cell, mean AF-intensity per cell, cell area and absolute numbers of M, L and ML per cell were reported. Also, for each of these cells, the (M+ML)/L-ratio was calculated, meaning that melanin containing granules predominate when >1, and pure L granules predominate when <1.

Statistical analysis

Data collection, organization and analysis was performed using SPSS statistic (IBM SPSS 25.0, IBM corporation, Armonk, NY, USA) and Microsoft office software packages

(Microsoft Corporation, Redmond, WA, USA). Categorical variables are presented as numbers and percentages, continuous variables are expressed as means ± standard deviation (STD).

Results

Data on total number of granules, cell area, number of granules per cell area, and (M + ML)/L-ratio in an average RPE cell related to age and the specific retinal location is reported in the Table 1 (11). For the current study, granule data of 420 RPE cells from 15 RPE/BrM flat mounts without retinal pathologies at three predefined locations (11) were included (total of 42 locations).

Characteristics of RPE cells with low or high granule load

RPE cells with low granule content (below the 5th percentile; total of 21 cells) were predominantly found within the >80 years group (14 of 21 cells) and at the fovea (11 fovea, 4 perifovea, 6 near periphery). Eight of these 21 cells are from the same donor (83 y/o female). RPE cells with low granule load are characterized by a high (M + ML)/L-ratio, a small cell area, and a low granule density, as compared to normal RPE cells at the respective locations (Table 1, Figure 1).

RPE cells with high granule content (above the 95th percentile; total of 21 cells) were predominantly found within the >80 years group (14 of 21 cells), and at the perifovea. Interestingly, none of these fully packed cells were found at the fovea (0 fovea, 14 perifovea, 7 near periphery). Six of the 21 cells are from the same donor (88 y/o male). RPE cells with high granule content are characterized by a low (M+ML)/L-ratio and a large cell area (Table 1, Figure 1).

Figure 2 displays the characteristics of those cells with high or low granule load. Those RPE cells with a high number of intracellular granules (>95th percentile) contained about two times more granules compared to an average RPE cell, and about six times more granules than an RPE cell below the 5th percentile, at the respective locations.

Characteristics of RPE cells with low or high AF-intensity

At each of the analyzed 42 locations, RPE cells with an AF-intensity 1.5 standard deviations lower or higher than the location's mean AF value were defined as cells with remarkably low or high AF-intensity, respectively. Twenty cells with low AF-intensity and twenty-eight cells with high AF-intensity were identified (Table 1).

RPE cells with low AF-intensity had about 300 granules in total (316.5±127.9), while RPE cells with high AF-intensity contained about 500 granules (499.6±359.3).

RPE cells with low AF-intensity were found at all three locations (5 fovea, 6 perifovea, 9 near periphery) and were distributed equally between the two age groups (10 ≤51 years group; 10 >80 years group). They were characterized by a high (M+ML)/L-ratio at all three locations (Table 1). Foveal and perifoveal RPE cells with low AF-intensity were smaller

than the average foveal and perifoveal RPE cell while cell area at near periphery was comparable with the average RPE cell at this location.

RPE cells with high AF-intensity were found at all three locations (8 fovea, 9 perifovea, 11 near periphery) and in both age groups (13 ≤51 years group; 15 >80 years group). They were characterized by a low (M+ML)/L-ratio and a cell area about the same size as an average RPE-cell (Table 1, Figure 3).

Discussion

Cells of the RPE can host hundreds of granules within their cell body, including granules of AF relevance (L, MLF, M) (11,16) and mitochondria (17). L and ML show AF properties after blue light excitation and are the major contributor to fundus AF (3). Elevated FAF has been linked to excessive L load of RPE cells and to subsequent development of AMD and RPE atrophy (18), though supporting histological evidence from well-characterized human eyes was lacking.

The results presented here confirm our previous data that L load seems to be regulated at a cellular level, at least in normal aging eyes, and to be related to topography of the overlying photoreceptors. While there is an increase in granule load with age, RPE cells that have massive L overload or significant increased granule density have not been found. Even those cells with the highest amount of L granules had only twice as many granules in their cell body as the average RPE cell at the respective location. The absolute number of granules per cell, however, has to be put in relation to the cell volume. In our study, the granule density of RPE cells with high granule content was in the same range as in an average RPE cell at the same location. Larger cells can contain a larger number of granules. Therefore, our observed absence of L-loaded cells at the fovea is not surprising since foveal RPE cells have a smaller area than RPE cells from outside the fovea.

Noticeable differences, however, were observed in granule density between RPE cells with low and high granule content. Cells with a high number of granules are more densely packed, despite the fact that they already have a larger area and volume. These tight packed RPE cells were predominantly located at the perifovea, probably resulting from intense rod photoreceptor-RPE cell interactions during the visual cycle and daily disk shedding with the subsequent deposition of lipofuscin granules (19). On the contrary, RPE cells with low granule content show predominately melanolipofuscin granules, a feature of foveal cells, as recently shown (11). Future studies could focus on the contribution of the different photoreceptor systems (cones versus rods) to lipofuscin accumulation within the RPE cells and whether lipofuscin originating from cone outer segment tips differs from that of rod outer segment tips. Imaging mass spectrometric studies of photoreceptors and RPE cells might further help to clarify this (20).

Only a few RPE cells showed increased/decreased AF intensities (above or below 1.5 standard deviations of the mean AF at the distinct location), as compared to the adjacent cells. This finding confirms that in healthy aging, AF signal arises equally from the different cells in a given location. However, regional differences are visible, as described *ex vivo*

(13,21) and *in vivo* (22,23), related to the proportion of L and ML granules and photoreceptor topography (24). Whether these findings can be confirmed in AMD eyes is basis of ongoing studies.

Massive lipofuscin load has been intensively discussed as a major contributor to the development of AMD (12). However, Rudolf *et al.* and others showed that the hyperautofluorescent signal in the junctional zone of geographic atrophy in late-stage non-neovascular AMD could be explained by the phenomena of stacked RPE cells, i.e., ectopic RPE cells that left the monolayer and migrated toward the inner retina, rather than individual RPE cells with massive granule load (14,25). Granule density in RPE cells with high AF in our study did not exceed the mean AF of an average RPE cell by more than a factor of 1.8, supporting the conclusions of Rudolf *et al.* (14).

Limitations of our study include the analysis of a small number of RPE cells per location. It cannot be excluded that results might differ in an analysis of larger sample sizes. The use of tissue of normal donor eyes does not allow any conclusions on RPE granule distribution in diseased eyes and its possible relationship to AMD; however, studies examining AMD tissues are currently being conducted in our lab.

Strengths of our analysis include RPE measurements at exactly predefined locations (13), especially in relation to the fovea and the overlying photoreceptor distribution.

Granule distribution data revealed that RPE cells with high granule content had only twice as many granules within the cell body as an average RPE cells. RPE cells with massive granule loads were not detectable. Also, intracellular granule type proportion seems to follow overlying photoreceptor distribution in that ML granules predominate in the fovea, with mostly cone photoreceptors, and L granules predominate in the perifovea, with mostly rod photoreceptors. These findings highlight the potential of RPE cells to regulate intracellular granule accumulation as part of their normal physiology. Variations in diseases like AMD are currently examined.

Acknowledgments

Funding:

Dr. Werner Jackstädt Foundation (TA), NIH/NEI 1R01EY027948 (TA, RH, CAC), 1R01EY06109 (CAC).

References

1. Pollreisz A, Neschi M, Sloan KR, et al. Atlas of Human Retinal Pigment Epithelium Organelles Significant for Clinical Imaging. Invest Ophthalmol Vis Sci 2020;61:13.
2. Feeney-Burns L, Berman ER, Rothman H. Lipofuscin of human retinal pigment epithelium. Am J Ophthalmol 1980;90:783–91. [PubMed: 7446665]
3. Delori FC, Goger DG, Dorey CK. Age-related accumulation and spatial distribution of lipofuscin in RPE of normal subjects. Invest Ophthalmol Vis Sci 2001;42:1855–66. [PubMed: 11431454]
4. Schmitz-Valckenberg S, Holz FG, Bird AC, et al. Fundus autofluorescence imaging: review and perspectives. Retina 2008;28:385–409. [PubMed: 18327131]
5. Delori FC, Dorey CK, Staurenghi G, et al. In vivo fluorescence of the ocular fundus exhibits retinal pigment epithelium lipofuscin characteristics. Invest Ophthalmol Vis Sci 1995;36:718–29. [PubMed: 7890502]

6. Lipofuscin Feeney L. and melanin of human retinal pigment epithelium. Fluorescence, enzyme cytochemical, and ultrastructural studies. Invest Ophthalmol Vis Sci 1978;17:583–600. [PubMed: 669890]
7. Weiter JJ, Delori FC, Wing GL, et al. Retinal pigment epithelial lipofuscin and melanin and choroidal melanin in human eyes. Invest Ophthalmol Vis Sci 1986;27:145–52. [PubMed: 3943941]
8. Ach T, Tolstik E, Messinger JD, et al. Lipofuscin redistribution and loss accompanied by cytoskeletal stress in retinal pigment epithelium of eyes with age-related macular degeneration. Invest Ophthalmol Vis Sci 2015;56:3242–52. [PubMed: 25758814]
9. Gliem M, Muller PL, Finger RP, et al. Quantitative Fundus Autofluorescence in Early and Intermediate Age-Related Macular Degeneration. JAMA Ophthalmol 2016;134:817–24. [PubMed: 27253610]
10. Orellana-Rios J, Yokoyama S, Agee JM, et al. Quantitative Fundus Autofluorescence in Non-Neovascular Age-Related Macular Degeneration. Ophthalmic Surg Lasers Imaging Retina 2018;49:S34–42. [PubMed: 30339266]
11. Bermond K, Wobbe C, Tarau IS, et al. Autofluorescent Granules of the Human Retinal Pigment Epithelium: Phenotypes, Intracellular Distribution, and Age-Related Topography. Invest Ophthalmol Vis Sci 2020;61:35.
12. Dorey CK, Wu G, Ebenstein D, et al. Cell loss in the aging retina. Relationship to lipofuscin accumulation and macular degeneration. Invest Ophthalmol Vis Sci 1989;30:1691–9. [PubMed: 2759786]
13. Ach T, Huisingh C, McGwin G Jr., et al. Quantitative autofluorescence and cell density maps of the human retinal pigment epithelium. Invest Ophthalmol Vis Sci 2014;55:4832–41. [PubMed: 25034602]
14. Rudolf M, Vogt SD, Curcio CA, et al. Histologic basis of variations in retinal pigment epithelium autofluorescence in eyes with geographic atrophy. Ophthalmology 2013;120:821–8. [PubMed: 23357621]
15. Schindelin J, Arganda-Carreras I, Frise E, et al. Fiji: an open-source platform for biological-image analysis. Nat Methods 2012;9:676–82. [PubMed: 22743772]
16. Pollreisz A, Messinger JD, Sloan KR, et al. Visualizing melanosomes, lipofuscin, and melanolipofuscin in human retinal pigment epithelium using serial block face scanning electron microscopy. Exp Eye Res 2018;166:131–9. [PubMed: 29066281]
17. Pollreisz A, Neschi M, Sloan KR, et al. Deciphering subcellular signal sources for optical coherence tomography (OCT) and autofluorescence (AF) imaging of the human retinal pigment epithelium (RPE). Invest Ophthalmol Vis Sci 2019;60:1574.
18. Dorey C, Staurenghi G, Delori F. Lipofuscin in aged and AMD eyes. Retinal degeneration. Boston, MA: Springer, 1993:3–14.
19. Crouch RK, Koutalos Y, Kono M, et al. A2E and Lipofuscin. Prog Mol Biol Transl Sci 2015;134:449–63. [PubMed: 26310170]
20. Anderson DMG, Messinger JD, Patterson NH, et al. Lipid Landscape of the Human Retina and Supporting Tissues Revealed by High-Resolution Imaging Mass Spectrometry. J Am Soc Mass Spectrom 2020. [Epub of print]. doi: 10.1021/jasms.0c00119.
21. Wing GL, Blanchard GC, Weiter JJ. The topography and age relationship of lipofuscin concentration in the retinal pigment epithelium. Invest Ophthalmol Vis Sci 1978;17:601–7. [PubMed: 669891]
22. von Rückmann A, Fitzke FW, Bird AC. Distribution of fundus autofluorescence with a scanning laser ophthalmoscope. Br J Ophthalmol 1995;79:407–12. [PubMed: 7612549]
23. Greenberg JP, Duncker T, Woods RL, et al. Quantitative fundus autofluorescence in healthy eyes. Invest Ophthalmol Vis Sci 2013;54:5684–93. [PubMed: 23860757]
24. Curcio CA, Sloan KR, Kalina RE, et al. Human photoreceptor topography. J Comp Neurol 1990;292:497–523. [PubMed: 2324310]
25. Zanzottera EC, Ach T, Huisingh C, et al. Visualizing Retinal Pigment Epithelium Phenotypes in the Transition to Geographic Atrophy in Age-Related Macular Degeneration. Retina 2016;36 Suppl 1:S12–25. [PubMed: 28005660]

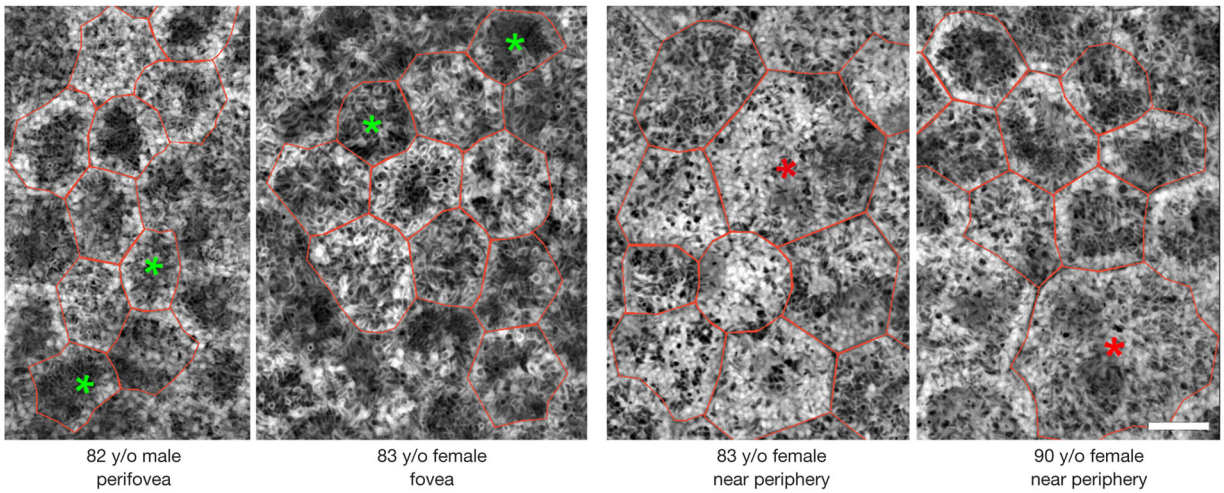

Figure 1.

Retinal pigment epithelium (RPE) cells with low/high granule load. The colored asterisks mark the cells with low (green) and high (red) amounts of granules. Individual RPE cells are red-rimmed. Structured Illumination Microscopy (summation of the whole image stack). Scale bar: 10 μm.

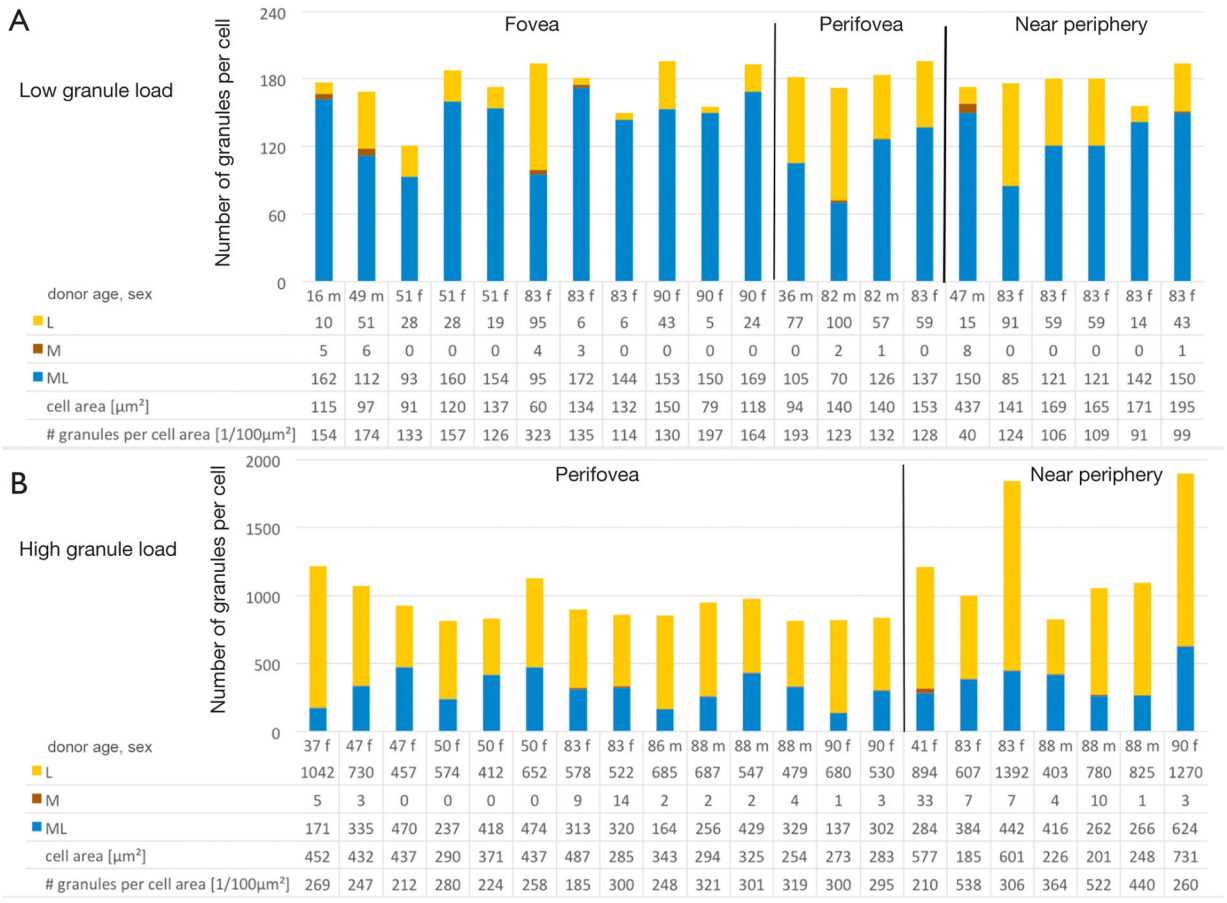

donor age, sex	16 m	49 m	51 f	51 f	51 f	83 f	83 f	83 f	90 f	90 f	90 f	36 m	82 m	82 m	83 f	47 m	83 f	83 f	83 f	83 f	83 f
L	10	51	28	28	19	95	6	6	43	5	24	77	100	57	59	15	91	59	59	14	43
M	5	6	0	0	0	4	3	0	0	0	0	0	2	1	0	8	0	0	0	0	1
ML	162	112	93	160	154	95	172	144	153	150	169	105	70	126	137	150	85	121	121	142	150
cell area [µm²]	115	97	91	120	137	60	134	132	150	79	118	94	140	140	153	437	141	169	165	171	195
# granules per cell area [1/100µm²]	154	174	133	157	126	323	135	114	130	197	164	193	123	132	128	40	124	106	109	91	99

donor age, sex	37 f	47 f	47 f	50 f	50 f	50 f	83 f	83 f	86 m	88 m	88 m	88 m	90 f	90 f	41 f	83 f	83 f	88 m	88 m	88 m	90 f
L	1042	730	457	574	412	652	578	522	685	687	547	479	680	530	894	607	1392	403	780	825	1270
M	5	3	0	0	0	0	9	14	2	2	2	4	1	3	33	7	7	4	10	1	3
ML	171	335	470	237	418	474	313	320	164	256	429	329	137	302	284	384	442	416	262	266	624
cell area [µm²]	452	432	437	290	371	437	487	285	343	294	325	254	273	283	577	185	601	226	201	248	731
# granules per cell area [1/100µm²]	269	247	212	280	224	258	185	300	248	321	301	319	300	295	210	538	306	364	522	440	260

Figure 2.

Characteristics of cells with low (A) high (B) granule load. F, female; m, male; L, lipofuscin; ML, melanolipofuscin; M, melanosomes. The Y-axis in A is only ~10% the height of the Y-axis in B.

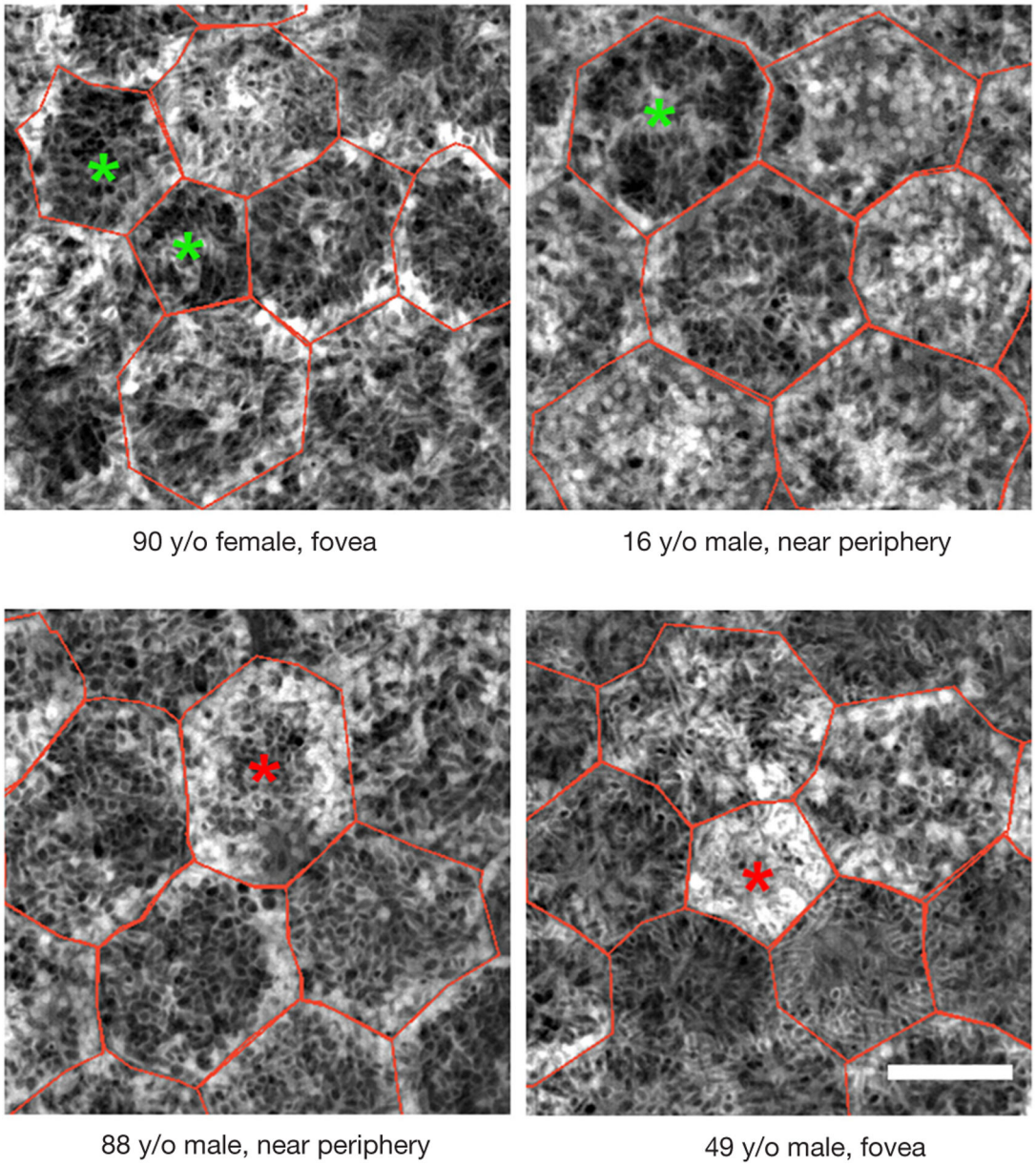

Figure 3.

Retinal pigment epithelium (RPE) cells with low/high autofluorescence (AF) intensity. The colored asterisks mark the cells with low (green) and high (red) total autofluorescence intensity. Individual RPE cells are red-rimmed. Structured Illumination Microscopy (summation of the whole image stack). Scale bar: 10 μm.

Table 1

Characteristics of RPE cells with extremes of granule load and autofluorescence (AF)

Location	Group	Characteristic	RPE-cells with				All RPE-cells
			Low granule content	High granule content	Low AF-intensity	High AF-intensity	
Fovea	≤51 years group	number of cells	n=5	n=0	n=2	n=6	n=70
		area [μm^2]	112.0±18.5	n/a	116.0±26.9	143.0±42.6	162.3±34.4
		(M+ML)/L-ratio	7.2 ±5.7	n/a	14.3±7.5	2.8±1.9	5.9±5.4
		number of granules per cell area [×/100 μm^2]	148.8 ±19.3	n/a	231.0±66.9	177.7±65.9	191.4±39.4
	>80 years group	number of cells	n=6	n=0	n=3	n=2	n=50
		area [μm^2]	112.2±35.3	n/a	117.0±18.5	181.0±36.8	172.3±57.8
		(M+ML)/L-ratio	15.8 ±13.4	n/a	10.3±11.9	2.1±1.4	4.9±6.6
		number of granules per cell area [×/100 μm^2]	177.2 ±77.4	n/a	143.3±20.6	201.3±89.3	204.7±53.1
Perifovea	≤51 years group	number of cells	n=1	n=6	n=3	n=2	n=80
		area [μm^2]	94.3	403.3±62.5	157.7±20.7	250.0±2.8	224.7±74.3
		(M+ML)/L-ratio	1.4	0.6±0.3	1.8±0.3	0.2±0.1	1.0±0.8
		number of granules per cell area [×/100 μm^2]	193.1	248.3±26.2	224.0±3.9	303.1±21.8	236.2±36.0
	>80 years group	number of cells	n=3	n=8	n=3	n=7	n=70
		area [μm^2]	144.1±7.6	317.9±73.8	143.7±11.0	204.1±47.7	215.9±65.6
		(M+ML)/L-ratio	1.8 ±0.9	0.5±0.2	1.6±1.1	0.4±0.2	0.7±0.4
		number of granules per cell area [×/100 μm^2]	127.7 ±4.3	283.8±45.7	178.8±87.1	247.5±45.5	230.4±52.6
Near periphery	≤51 years group	number of cells	n=1	n=1	n=5	n=5	n=80
		area [μm^2]	437.3	576.5	194.8 ±48.3	182.2±56.6	214.0±63.4
		(M+ML)/L-ratio	10.5	0.4	2.5±1.8	0.8±0.4	1.6±1.4
		number of granules per cell area [×/100 μm^2]	39.6	210.1	221.3±57.2	217.9±62.0	194.0±36.4
	>80 years group	number of cells	n=5	n=6	n=4	n=6	n=70
		area [μm^2]	168.3±19.2	365.5±237.3	200.3±61.8	276.2±217.8	2151±89.7
		(M+ML)/L-ratio	3.7±3.7	0.5±0.3	4.0±4.2	0.6±0.3	1.5±1.6
		number of granules per cell area [×/100 μm^2]	106.1±12.3	405.1±114.3	175.8±79.0	280.5±163.4	228.6±87.4

L, lipofuscin; ML, melanolipofuscin; M, melanosomes. (M+ML)/L-ratio, melanin containing granules predominate when >1, and pure L granules predominate when <1.